ISSN:2790-1688 DOI: 10.56028/aetr.2.1.514

Calibration Method of Normal Critical Damping Ratio in Particle Discrete Element Rock Model

Zehua Zhang

College of Pipeline and Civil Engineering, China University of Petroleum (East China), Qingdao, China, 266580

583365895@qq.com

Abstract. The calibration of dynamic mesoscopic parameters such as the normal critical damping ratio will directly affect the simulation results when wave velocity dynamic analysis is carried out on the particle discrete element rock model. This paper presents a fast calibration method for the normal critical damping ratio in the particle discrete element model. Firstly, the relationship between the normal critical damping ratio and the model energy attenuation rate is quantitatively analyzed based on the fundamental theory of discrete particle elements and energy conservation law. Then, based on the rock model with determined macroscopic mechanical parameters, the elastic longitudinal wave test is carried out to study the influence of the model energy attenuation rate with a normal critical damping ratio. The theoretical formula is modified according to the numerical results. Finally, the calibration formula of the normal critical damping ratio in the discrete particle element model is given. It is a new method to calibrate the normal critical damping ratio of the discrete particle model quickly and conveniently by using the theory of discrete particle elements and energy. It can provide a reference for constructing an accurate particle discrete element rock model.

Keywords: Normal critical damping ratio; Model energy attenuation rate; Particle discrete element; Calibration method

1. Introduction

As a common natural phenomenon, wave propagation and attenuation in rock media is a hot and difficult point in rock mechanics. The study of rock wave velocity is widely used in engineering practice, such as nondestructive testing of rock medium, prediction of vibration velocity under impact loads, and micro-structure changes of rock interior. Therefore, many experiments and numerical simulations have been carried out on rock wave velocity.

For the study the rock wave velocity test, Reza Khajevand et al.[1] collected 15 various sedimentary rock samples of four rock types and conducted a comprehensive laboratory test. Empirical equations were developed using regression analyses between P wave velocity and the measured properties. The obtained results showed that all properties strongly correlated to P wave velocity. Charalampos Saroglou[2] determined the fracture mechanism and the effect of fracturing degree. Samples were loaded at certain percentages of peak strength, and ultrasonic wave velocity was recorded after every test. It proved that the wave velocity decreases exponentially with increasing fracturing degree. J. Vilhelm et al.[3] used pulse- transmission technique to determine the field and the laboratory velocities of P and S waves, special measurements using neutron diffraction were carried out, making it possible to establish the influence of mineral crystallographic preferred orientations (CPOs) of bulk rock sample on elastic wave propagation and its anisotropy.

Particle discrete elements originated in the United States. In 1979, Cundall and Strack[4] developed the first two-dimensional discrete element simulation program to study the mechanical behavior of granular media, which began the discrete element simulation of particle motion. D.O.Potyondy, P.A.Cundall[5] believed that rock is like a collection of cemented particles composed of particles with complex shapes. The particles and bonds are deformable and may break. N.Cho, C.D. Martin, and DC Sego[6] used PFC to establish a rock particle model and calibrate the micro-parameters of the model through rock uniaxial tests in the laboratory.

ISSN:2790-1688 DOI: 10.56028/aetr.2.1.514

To solve the problem of dynamic mesoscopic parameters calibration, this paper is based on the theoretical derivation of the energy conservation law. Particle discrete element theory and the numerical test of the elastic longitudinal wave of particle discrete element model of rock reveals the energy attenuation of elastic wave in the particle discrete element model mesoscopic mechanism and quantifies the relationship between model dynamic mesoscopic parameters and energy attenuation rate per unit volume, finally provides a calibration method for the normal critical damping ratio in the particle discrete element model. Due to the relatively easy realization of wave velocity measurement in engineering practice, this method can be used to quickly and conveniently determine the normal critical damping ratio according to the field wave velocity measurement and establish an accurate particle discrete element model, to provide a basis for the in-depth study of wave propagation and attenuation law in rock.

2. Methodology

2.1 Energy dissipation mechanism of parallel bonding contact model

In the particle discrete element model, The energy is dissipated by the contact model and friction. However, these dissipative mechanisms may not be sufficient to obtain a steady-state solution in a reasonable time. Local damping is used to remove additional kinetic energy. Local damping is applied to each particle or cluster, and the damping force is proportional to the unbalanced force. For the compact particle model, non-zero local damping can be used to establish equilibrium and quasi-static deformation simulation. However, in the dynamic analysis, the energy in the model system should be dissipated based on the viscous damping of the contact model, and the local damping should be set to 0.

The parallel bonding contact model can be used as a common contact model to simulate the mechanical behavior of rock and soil materials because it provides the mechanical behavior of cement-like bonding between two finite-size contact surfaces. The energy stored in the parallel bonding model is divided into four parts: The strain energy stored in the linear spring Ek; Inter-particle friction energy dissipation Ef; The viscous damping energy dissipation of parallel bond contact ED. the bond strain energy stored in the parallel bond spring $\overline{E_k}$.

The viscous damping of parallel bonding contact is the main energy dissipation path, and the viscous damping coefficient can be divided into normal and shear damping coefficients[7] :

$$c_n = 2\beta_n\sqrt{mk_n} \qquad (2.1)$$

$$c_s = 2\beta_s\sqrt{mk_s} \qquad (2.2)$$

Where cn and cs are the normal and shear viscous damping coefficients, respectively; βn and βs are the normal and shear critical damping ratio in the model, respectively; and kn and ks are the normal and shear stiffness of the parallel bonding contact, respectively.

From the normal and shear viscous damping coefficients, the critical viscous damping coefficient c0 of parallel bonding contact can be obtained as:

$$c_0 = \sqrt{c_n^2 + c_s^2} = 2\sqrt{m\left(\beta_n^2 k_n + \beta_s^2 k_s\right.} \qquad (2.3)$$

2.2 Particle discrete element model energy dissipation theory

When the elastic longitudinal wave incident particle discrete element rock model, the energy of the whole model system can be divided into four parts [8]: incident wave energy EI., reflected wave energy ER., transmitted wave energy ET, and rock deformation energy ES. The rock deformation energy ES includes two energy parts: releasable deformation energy Ee and dissipated energy EL. The released deformation energy Ee is composed of linear strain energy Ek and bonding strain energy $\overline{E_k}$ in the model. In contrast, the dissipated energy EL in the model is divided into

ISSN:2790-1688 DOI: 10.56028/aetr.2.1.514
inter-particle friction energy Ef and viscous damping energy ED. The energy of the four parts is a function of time, namely EI (t), ER (t), ET (t), and ES (t). The whole system is an adiabatic closed system. According to the energy conservation principle, the incident wave energy EI (t) will all be converted into the energy of the remaining three parts:

$$E_I(t) = E_R(t) + E_T(t) + E_S($$ (2.4)

Where t is the time when the incident wave energy is completely dissipated in the model. Since the dispersion boundary was set on the right edge of the rock model, the wave energy at this boundary is all absorbed by the boundary particles, it can be considered that there is no reflection effect, so the reflected wave energy ER is not considered. It is assumed that all the releasable deformation energy Ee in the rock mass model is released. Since the incident wave is an elastic longitudinal wave, it will not cause the model to crack and fail, so the friction between particles, Ef=0, causes no energy dissipation. Finally, the rock deformation energy ES equals the model's viscous damping energy dissipation ED. The incident wave energy EI, transmitted wave energy ET, and viscous damping energy dissipation ED can be expressed as:

$$E_I(t) = \int_0^t \frac{1}{2} m_1 v_1^2(t) dt$$ (2.5)

$$E_T(t) = \int_0^t \frac{1}{2} m_2 v_2^2(t) dt$$ (2.6)

$$E_D(t) = \int_0^t c v_1^2(t) dt$$ (2.7)

Equation 2.5~2.7 can be substituted into Equation 2.4 to obtain:

$$\int_0^t \frac{1}{2} m_1 v_1^2(t) dt - \int_0^t c v_1^2(t) dt = \int_0^t \frac{1}{2} m_2 v_2^2(t)$$ (2.8)

Where m1 is the particle's mass at the incident boundary; m2 is the particle's mass at the transmission boundary; v1 is the incident wave velocity; v2 is the transmission wave velocity; c is the damping coefficient.

m is the mass per unit volume of the model. Taking m1=m2=m, Equation 2.8 can be transferred to

$$c = \frac{m \int_0^t \left[v_1^2(t) - v_2^2(t) \right] dt}{2 \int_0^t v_1^2(t) dt}$$ (2.9)

The basic motion equation of discrete particle element is [9] :

$$mx''(t) + cx'(t) + kx(t) = f($$ (2.10)

Where x is displacement; k is the stiffness coefficient; f is the external load on particles, and no external load is applied in the elastic longitudinal wave test system of particle discrete element rock model, that is, f=0.

It is assumed that the free vibration generated by the elastic longitudinal wave propagating in the model is critically damping, so the damping ratio ξ=1. According to Equations 2.9 and 2.10, the following can be obtained:

$$\xi = \frac{c}{c_0} = \frac{\sqrt{m} \int_0^t \left[v_1^2(t) - v_2^2(t) \right] dt}{4 \sqrt{\left(\beta_n^2 k_n + \beta_s^2 k_s \right)} \int_0^t v_1^2(t) dt} =$$ (2.11)

Energy attenuation rate is defined as [10] :

ISSN:2790-1688 DOI: 10.56028/aetr.2.1.514

$$\eta = \frac{\frac{1}{2}\int_0^t \left[mv_1^2(t) - mv_2^2(t)\right]dt}{\frac{1}{2}\int_0^t mv_1^2(t)dt} = \frac{\int_0^t \left[v_1^2(t) - v_2^2(t)\right]d}{\int_0^t v_1^2(t)dt} \quad (2.12)$$

If Equation 2.12 is substituted into Equation 2.11, the following can be obtained:

$$\eta = 4\sqrt{\frac{\beta_n^2 k_n + \beta_s^2 k_s}{m}} \quad (2.13)$$

According to Equation 2.13, the theoretical value of energy attenuation per unit volume under the action of each model parameter can be calculated.

3. Numerical simulation and results

3.1 The establishment of a numerical model

According to the International Society of Rock Mechanics (ISRM) regulations, the rock model specimen with a height to diameter of 2.5:1 were made using PFC2D, which were 50mm wide and 125mm high. A parallel bonding model was selected for the contact model, and 1720 particles were generated. The microscopic parameters of the model are shown in Table 3.1. The specimen of the established uniaxial compression model is shown in Figure 3.1.

Table 3.1 Mesoscopic parameters of rock model

Model	Parameter name	Variable parameter	Numerical value
Particle/ Linear bond part	cm_Dup	Largest radius /mm	2.49
		Particle diameter ratio	1.66
	lnm_emod/ pbm_emod	Elasticity modulus /GPa	55
	lnm_krat/ pbm_krat	Stiffness ratio	1.0
	lnm_fric/ pbm_fric	Friction coefficient	0.4
	kn	Normal stiffness/GPa	1
Parallel bond part	pbm_bemod	Elasticity modulus /GPa	55
	pbm_bkrat	Stiffness ratio	1.0
	pbm_ten_m	Mean normal strength /MPa	70
	pbm_coh_m	Mean shear strength /MPa	150
	pbm_fa	Internal friction angle /°	30

During the numerical simulation, the loading wall should be strong enough to ensure that particles will not damage it. The effective modulus of the wall was set to 100 GPa, and the loading rate was 0.05s-1. The uniaxial compression test is carried out on the generated rock model. The loading is suspended when the model stress decreases to 80% of the peak stress. The deviator stress-axial strain curve obtained from the uniaxial compression numerical test is shown in Figure 3.3. The macroscopic mechanical parameters of the rock model are shown in Table 3.2.

ISSN:2790-1688 DOI: 10.56028/aetr.2.1.514

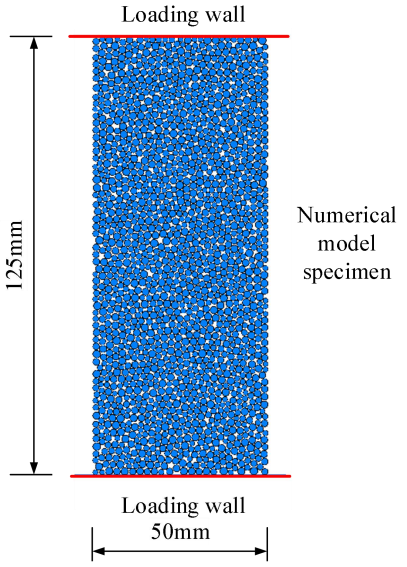

Fig. 3.1 Uniaxial compression model

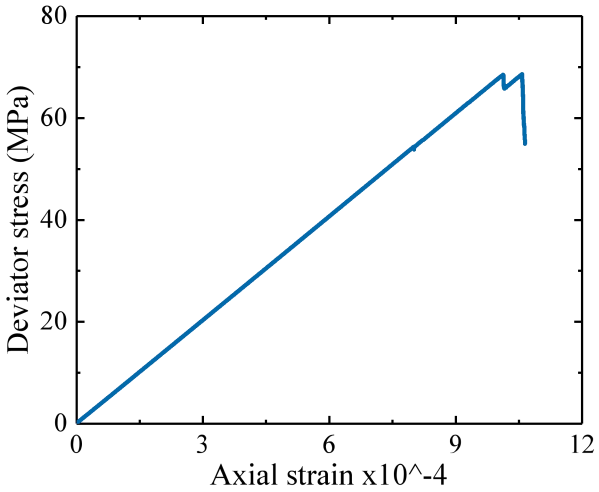

Fig. 3.2 Deviator stress - axial strain curve

Table 3.2 Macroscopic mechanical parameters of rock model

Parameter	Uniaxial compressive strength/MPa	Density/（kg/m3）	Poisson's ratio	Elasticity modulus/GPa	Internal friction angle/°
Value	68.60	2500	0.25	67.80	30

3.2 Implementation of numerical simulation

The numerical model adopted the viscous boundary proposed by LYsmer[11] and considered the diffusion effect of stress wave propagation at the boundary of rock mass proposed by Shi [12].

The relation between boundary force and particle velocity is:

$$F = -2\rho\, Cvr \tag{3.1}$$

Where r is the particle radius; ρ is the rock medium density; C is the wave velocity; v is the particle velocity.

$$F = \begin{cases} -\xi \cdot 2\rho\, C_p v_n r & \text{（Normal Boundary Force} \\ -\eta \cdot 2\rho\, C_s v_s r & \text{（Shear Boundary Force} \end{cases} \tag{3.2}$$

Where, ξ and η are the correction coefficient of longitudinal wave and shear wave dispersion effects, respectively.

The incident wave is a half sine wave, and the half sine wave equation is

$$v_1 = 0.01\left(1-\cos\left(2\pi f t_0\right)\right)/ \tag{3.3}$$

Where, v1 is the incident wave velocity; f is the frequency of the incident wave, f=100 Hz; t0 is the duration of the incident wave, t0=10ms.

ISSN:2790-1688 DOI: 10.56028/aetr.2.1.514

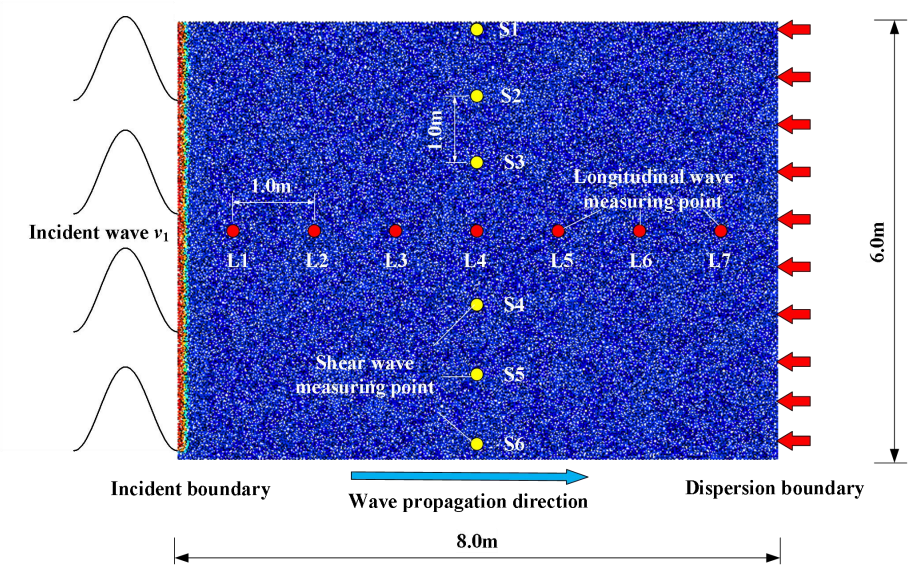

Fig. 3.3 Elastic longitudinal wave test system for particle discrete element rock numerical model

Using the microscopic parameters in Table 3.1, the servo generates a rock numerical model with a length of 8m and a width of 6m. The elastic longitudinal wave test system for discrete particle elements rock numerical model, as shown in Figure 3.3, is established. The left side of the model is the incident wave boundary. The monitoring points L1~L7 of longitudinal wave velocity are arranged along the direction of wave propagation. The monitoring points S1~S6 of shear wave velocity are arranged perpendicular to the direction of wave propagation. In order to avoid the influence of the reflection of elastic longitudinal waves on the monitoring point at the free surface, a diffusion boundary is applied to the right boundary of the rock model. The semi-sine wave is imported from the left side of the model, the normal critical damping ratio is adjusted, and the influence of the critical damping ratio on the energy dissipation law of elastic longitudinal wave propagating in the rock mass model is studied according to the monitoring data of each longitudinal measurement point.

Influence of normal critical damping ratio on energy dissipation of elastic longitudinal wave

The shear critical damping ratio βs is set as 0.5, and the numerical simulation is carried out according to the elastic longitudinal wave test of discrete elements of rock particles designed in Figure 3.3. Since the normal critical damping ratio βn is specified in PFC as [0,1], the case of no normal damping when βn is equal to 0 and the case of maximum normal damping when βn is equal to 1, causing waveform distortion are temporarily ignored. Therefore, the value of βn is adjusted within the range of [0.01,0.99]. Ninety-nine tests were conducted, and the energy attenuation rate per unit volume after each test was recorded. Figure 3.4 and 3.5 show the time-varying curves of particle velocity monitored by longitudinal measuring points L1~L7 and shear measuring points S1~S6 when the normal critical damping ratio βn and shear critical damping ratio βs are 0.5. The illustration in Figure 3.5 shows the enlarged waveform from 39ms to 43ms.

As shown in Figures 3.4 and 3.5, in the process of elastic longitudinal wave propagation, it can be assumed that the longitudinal wave waveform remains unchanged with the half-sine wave. The transverse dispersion effect can be ignored so that the energy attenuation rate η can be further simplified.

ISSN:2790-1688 DOI: 10.56028/aetr.2.1.514

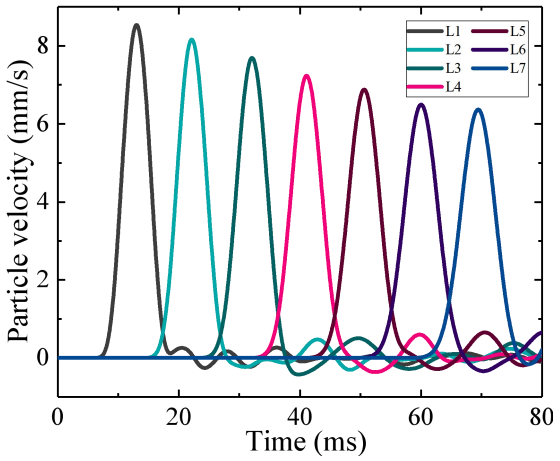

Fig. 3.4 Particle velocity-time curve of measured points L1~L7

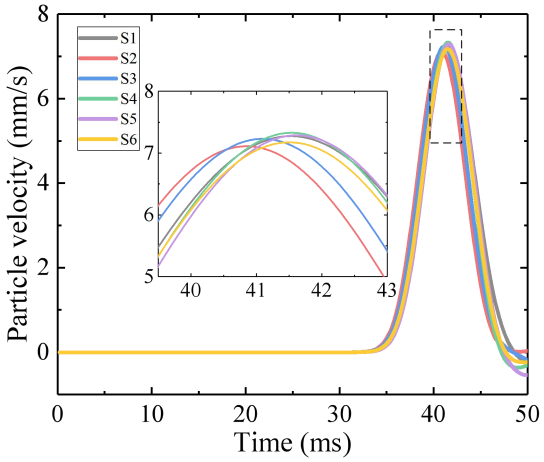

Fig. 3.5 Particle velocity-time curve of measuring points S1~S6

The incident wave is a half sine wave, and the incident wave equation is simplified as follows:

$$v_1 = 0.01\left(1-\cos\left(2\pi f t_0\right)\right)/2 = v_{\max} v(t_0 \tag{3.4}$$

Where, vmax is the peak value velocity of the incident wave, and v(t0) is the half-sine waveform function of the incident wave.

$$\eta = \frac{\int_0^t \left[v_1^2(t) - v_2^2(t)\right]dt}{\int_0^t v_1^2(t)dt} = \frac{\left(v_{1,\max}^2 - v_{2,\max}^2\right)\int_0^t v^2(t_0)dt}{v_{1,\max}^2 \int_0^t v^2(t_0)dt} = \frac{v_{1,\max}^2 - v_{2,\max}^2}{v_{1,\max}^2} \tag{3.5}$$

Where, v1max is the peak wave velocity of the measuring point; v2max is the peak wave velocity of the next adjacent measuring point along the wave propagation direction.

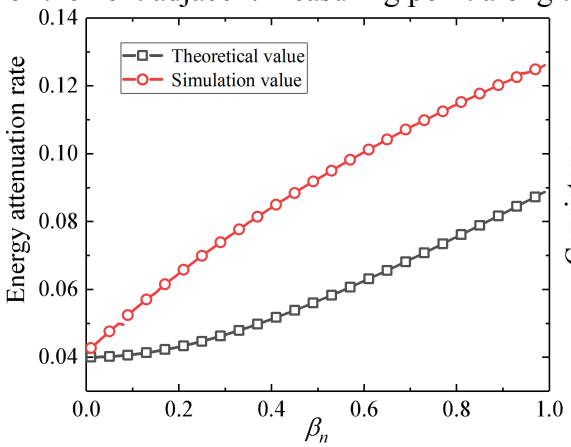

Fig. 3.6 Theoretical and numerical simulation -- energy attenuation rate curve

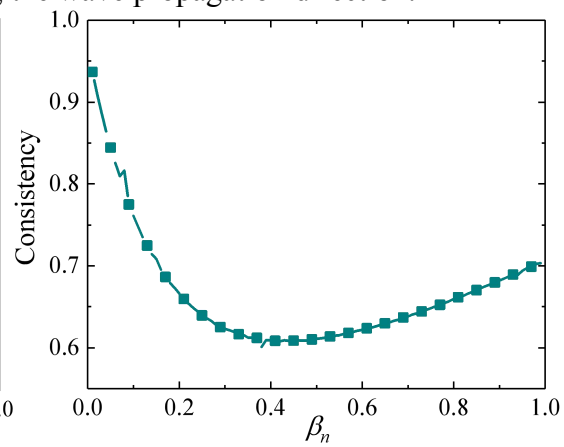

Fig. 3.7 Energy attenuation rate consistency curve

According to Equation 3.5, the energy attenuation rate of adjacent measuring points in each test group is calculated. The energy attenuation rate of each adjacent measuring point is averaged, that is, the energy attenuation rate per unit volume of the model under the action of the normal critical damping ratio. Consistency is the ratio of the theoretical value of energy attenuation per unit volume of the model to the simulated value. Under different normal critical damping ratios βn, the model's numerical simulation and theoretical energy attenuation per unit volume results and the consistency between the theory and the numerical simulation are shown in Figures 3.6 and 3.7.

As shown in Figure 3.6, under the action of microscopic parameters, only the influence of energy dissipation of the model of normal critical damping ratio is considered in this paper. When the value of normal critical damping ratio βn is within the range of [0.01,0.99], the numerical simulation value of energy attenuation rate per unit volume is within the range of [4.27%,12.61%], while the

ISSN:2790-1688 DOI: 10.56028/aetr.2.1.514
theoretical value is within the range of [4.00%,8.87%]. And the energy attenuation rate increased as the βn. As shown in Figure 3.7, the theoretical value of energy attenuation rate per unit volume is consistent with the simulated value by more than 60%. The consistency is high at both ends of the value range of βn. There is a certain error between the theoretical value and the numerical simulation value, which may be caused by the inevitable porosity of the particle discrete element model. When the normal critical damping ratio βn is 0, supplementary numerical simulation is carried out. The model's energy attenuation rate per unit volume is 4.20%. This part of energy consumption can be regarded as the initial parameters, such as model porosity. By increasing the influence of the initial parameters of the model, the calibration formula of Equation 2.13 is modified:

$$\eta_m = \eta_\beta + \eta_0 = \beta_n \left(4\sqrt{\frac{\beta_n^2 k_n + \beta_s^2 k_s}{m}} \right) + \eta_{\beta_n=0} \tag{3.6}$$

Where, ηm, ηβ, and η0 are correction values of energy attenuation rate per unit volume, contribution values of normal critical damping ratio to energy attenuation rate per unit volume, and contribution values of initial parameters of the model to energy attenuation rate per unit volume respectively; ηβ=0 is the energy attenuation rate per unit volume when the normal critical damping ratio is 0.

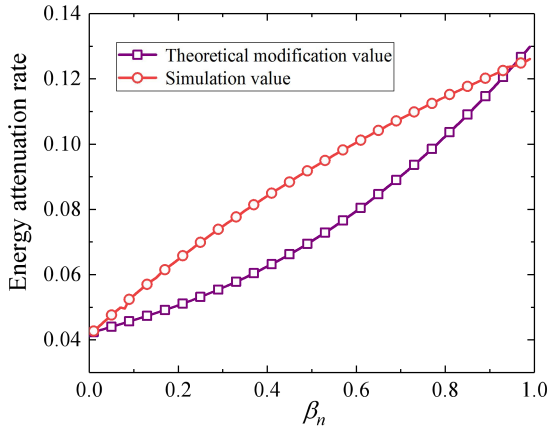

Fig. 3.8 Modified curve of energy attenuation rate of theoretical and numerical simulation

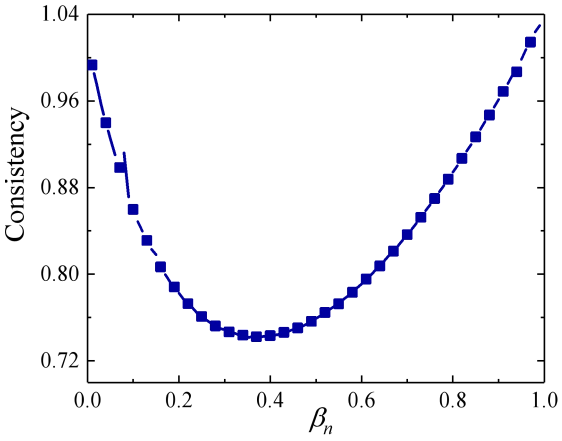

Fig. 3.9 Modified consistency curve

As shown in Figures 3.8 and 3.9, after the modification of increasing the influence of the initial parameters of the model, the coincidence degree is over 72%, which is more than 10% higher than before the modification. Therefore, the model's normal critical damping ratio can be calculated more accurately. According to the research results, the model's energy attenuation rate per unit volume should be determined when the normal critical damping ratio is 0. The energy attenuation rate per unit volume is determined according to the field wave velocity test. Then, Equation 3.6 is used to estimate the value of the model's normal critical damping ratio. Then the value is adjusted according to the relationship of consistency. When the simulated value of energy attenuation per unit volume is the same as the experimental value, the calibration of the normal critical damping ratio is completed.

4. Conclusion

Based on the theory of particle discrete element and energy principle, a calibration method for the normal critical damping ratio in the particle discrete element model is established in this paper. It can be used to quickly and conveniently determine the normal critical damping ratio in combination with the rock wave velocity test, which is easily realized in the field. Finally, the

ISSN:2790-1688 DOI: 10.56028/aetr.2.1.514
particle discrete element model can be established accurately and reliably. The main conclusions are as follows:

(1) Before calibrating the dynamic parameters such as the normal critical damping ratio, the normal and shear stiffness, and the normal and shear bonding strength of the parallel bonding contact in the particle discrete element model should first be calibrated according to the macroscopic mechanical parameters such as the uniaxial compressive strength and elastic modulus of the rock sample to be measured. The calibration of dynamic mesoscopic parameters is completed based on establishing an accurate static numerical model. If the calibration of dynamic parameters such as the normal critical damping ratio is completed first, and then the calibration of static mesoscale parameters such as the normal stiffness is carried out, according to the theoretical formula, the energy attenuation rate that has been calibrated will change, resulting in the inaccuracy of the constructed rock model.

(2) This paper provides a calibration method for the normal critical damping ratio in the particle discrete element model. Firstly, the energy attenuation rate per unit volume of the particle discrete element model should be simulated when the normal critical damping ratio is 0. Then, according to the energy attenuation rate of rock per unit volume measured by the elastic longitudinal wave propagation test in the rock, the theoretical value of the normal critical damping ratio is calculated from the revised theoretical formula as the value of βn in the model. And then, the value of βn is adjusted according to the consistency relation given in the paper. Finally, a numerical model of energy attenuation rate per unit volume is obtained, consistent with the actual rock, so that the subsequent rock model dynamics tests can be performed more reliably.

(3) When the elastic longitudinal wave propagation test is carried out in the rock, the energy attenuation rate per unit volume of the rock is substituted into the modified calibration formula of βn. Suppose the calculated value of βn is greater than 1. In that case, the model's viscous damping alone cannot complete the energy consumption. Therefore, in the particle discrete element model, we should consider the normal critical damping ratio βn and the influence of initial mesoscopic parameters such as model porosity on energy attenuation per unit volume.

Reference

[1] Reza,Khajevand.; Davood,Fereidooni. Assessing the empirical correlations between engineering properties and P wave velocity of some sedimentary rock samples from Damghan, northern Iran. Arabian Journal of Geosciences (2018) 11:528

[2] Charalampos,Saroglou.; Vasileios,Kallimogiannis. Fracturing process and effect of fracturing degree on wave velocity of a crystalline rock. Journal of Rock Mechanics and Geotechnical Engineering,2017,9(5).

[3] J,Vilhelm.; T,Ivankina.; T,Lokajíček.; V,Rudajev. Comparison of laboratory and field measurements of P and S wave velocities of a peridotite rock. International Journal of Rock Mechanics and Mining Sciences,2016,88.

[4] CUNDALLPA.; STRACKODL. A discrete numerical mode for granular assemblies. Geotechnique, 1979,29(1):47-65.

[5] D,O.Potyondy.; P,A.Cundall. A bonded-particle model for rock. International Journal of Rock Mechanics and Mining Sciences,2004,41(8).

[6] N,Cho.; C,D.Martin.; D,C.Sego. A clumped particle model for rock. International Journal of Rock Mechanics and Mining Sciences,2007,44(7).

[7] Cundall,P.A.; Strack,ODL. A discrete numerical model for granular assemblies.. Geotechnique . 1979

[8] Lifan,Rong.; Jianchun,Li.; Haibo,Li.; Zhiwen,Li.; Shengnan Hong. Experimental Research on Measuring Quality Factors of Jointed Rock Mass Based on Energy Method. Journal of Rock Mechanics and Engineering,2017,36(10):2474-2483.

[9] PFC 5.0 manual. Minneapolis,MN,USA: Itasca Consulting Group,2015

ISSN:2790-1688 DOI: 10.56028/aetr.2.1.514
[10] Wenzhen,Zhong.; Kejing,He.; Zhaoyao,Zhou.; Wei,Xia.; Yuanyuan,Li. Calibration of Damping Coefficient in Particle Discrete Element Simulation. Acta Physica Sinica,2009,58(08):5155-5161.

[11] MAHABADIO,K.; LISJAK,A.; MUNJIZA,A. Y-Geo: New combined finite-discrete element numerical code for geomechanical applications. International Journal of Geomechanics, 2012, 12(6): 676－688.

[12] Particle flow (PFC5.0) numerical simulation technology and its application. China Architecture & Building Press, Chong Shi,2018.